Structural, Dynamic, and Thermodynamic Study of KF–AlF 3 Melts by Combining High-Temperature NMR and Molecular Dynamics Simulations

Kelly Machado, Didier Zanghi, Mathieu Salanne, Catherine Bessada

Structure, dynamics and thermodynamic study of KF-AlF_3 melts by combining high temperature NMR and molecular dynamics simulations

Kelly Machado[a], Didier Zanghi[a], Mathieu Salanne[b] and Catherine Bessada[a]

[a]CEMHTI UPR3079 CNRS, Univ. Orléans, F-45071 Orléans, France

[b]PHENIX UMR 8234 CNRS, Univ. Paris, F75005 Paris, France

*corresponding author: kelly.machado@cnrs-orleans.fr

Abstract

Molten cryolite (NaF-AlF_3) plays a key role for aluminum production since it is used as a solvent. Among the various leads to improve the electrochemical processes, adding other fluoride salts is one of the most promising. However there is very few data on the impact of these additional species on the physico-chemical properties of the melt. In order to fill this gap we investigate the properties of high temperature KF-AlF_3 liquids by combining NMR spectroscopy, molecular dynamics and DFT calculations. Our results show that the speciation, and consequently the transport properties differ from that of cryolite. This work will allow to assess the interest of adding KF in aluminium production processes.

1. Introduction

Nowadays, in aluminium industrial process, the electrolyte is a fluoride mixture at around 965°C mainly composed by NaF, AlF_3, Al_2O_3 and CaF_2. Different cryolite ratios ($\%\, mol\ NaF/\%\, mol\ AlF_3$) and additives can be present during the process and change significantly the physical-chemical properties of the electrolyte. All these modification have an impact on the process of aluminium production. To improve the chemical and physical properties of the fluoride melts used on aluminium production, the alkali effect has been studied by different authors [1–4]. The objective is to find the electrolyte composition that decrease the melting point and aluminium solubility, improve the dissolution rate of aluminium oxide in the electrolyte and the electric conductivity [2,5]. In order to reduce the operating temperature potassium fluoride is the most attractive. The substitution of sodium by potassium in the system allows a temperature drop between 10 and 280°C depending on the AlF_3 concentration. It has been also claimed that it increases the alumina solubility [1,4–8].

Nevertheless potassium fluoride shows also to be destructive to the carbon cathode due to the expansion of potassium inside the cathode [7,9]. Only low KF concentrations are acceptable in the electrolyte and the composition based on NaF-KF-AlF_3 is considered as a promising electrolyte system for low temperature aluminium electrolysis [3].

The phase diagram of KF-AlF_3 has been determined by several workers [5,10] and two compounds have been identified : K_3AlF_6 and $KAlF_4$. However some gaps can be found for the melting points as well as some discrepancies between the reported values: for K_3AlF_6 the difference can reach as much as 50°C [10–12]. The study of these molten salts is very difficult experimentally because of their higher melting point and their corrosive behavior. Despite the experimental difficulties, spectroscopy techniques such as Raman and NMR have been used to describe the structure of such melts [1,13–15]. Tixhon et al [8] and Robert et al [16] performed Raman studies in KF-AlF_3 melts. Their works both demonstrated that the major entities are free fluorine, AlF_5^{2-} and AlF_4^- with minor amounts of AlF_6^{3-}. The larger size of the cation was claimed to stabilize the AlF_5^{2-} fluoroaluminate with respect to NaF-AlF_3 melts.

The aim of this present paper is to go further in describing the structure of KF-AlF_3 system and to compare it with previous results [17] for the system NaF-AlF_3. By combining high temperature NMR and molecular dynamics, it is possible to propose a complete picture of the liquid and of its properties.

2. Experimental and simulation section

2.1 High temperature NMR experiments

NMR experiments were performed using a Bruker AVANCE I spectrometer operating at 9.4T coupled to a CO_2 laser heating system [14,17–19] that allows us to record the NMR spectra at high temperature. The measurements were carried out at 1305 K and/or at 20K above the melting point.

All samples were prepared in a glove box under dried argon by mixing proportions of AlF_3 (Alfa Aesar 99.99 %), KF (Alfa Aesar, 99.99%) and introduced in a high purity boron nitride crucible closed by a screw cap. During the NMR experiments at high temperature the crucibles were under argon atmosphere to avoid the oxidation. The crucibles are introduced in a modified axial Bruker NMR probe, and two continuous CO_2 laser irradiates the bottom and the top of the crucible. A calibration curve between the temperature and the laser power is systematically performed before the experiments. For this purpose, fluorinated pure compounds whose melting points are known have been used. Then for each samples, NMR

spectra are recorder after 5 min at the desired temperature using a single pulse (90°) experiment. The ^{27}Al and ^{19}F chemical shifts are referenced to 1 M $Al(NO_3)$ and CFCl, respectively.

2.2 Polarizable ion model

As in previous studies [17], we simulated the molten fluoride by classical molecular dynamics simulations in the NVT microcanonical ensemble using a Nosé-Hoover thermostat after an initial stage of equilibration in the NPT ensemble at the atmospheric pressure. To achieve that outcome, we developed a classical polarizable interaction potential able to account the interatomic interactions in these ionic compounds. Most of the short-range structural properties can be attributed to the competition between the overlap repulsion due to the Pauli principle and the Coulombic interaction. The addition of the dispersion contribution due to the correlated fluctuations of the electrons results in introducing an attractive effect between the ions to better reflect the thermodynamic properties for instance.

Compared to the classical rigid ion existing models, this polarizable ion model takes also into account the effects arising from the polarization of each ion which is the response of the electron cloud of the ion to the local electric field. The inclusion of the polarization effects in the interaction potential is crucial for describing the transport properties (conductivity and viscosity) and the lifetimes of the coordination complexes present in the melts together with the degree to which theses anionic species are linked together to form a network [20]. The total energy arising from these four terms (repulsion, Coulomb, dispersion and polarization) can be written as a sum over all the pairs of ions [21,22].

All the parameters of this interatomic potential are obtained by an adjustment procedure described in previous work [17]. This parametrization is based on first principles calculations using the density functional theory approach implemented in the code VASP [23,24].

The potential parameters obtained are grouped in table 1. For a constant charge radius, an increase of the ion polarization is expected intuitively with size of the ion. This is indeed verified, in our previous study for NaF-AlF_3 system [17] the Na^+ ion had a polarizability (0.9 a.u.) substantially lower than the one obtained for K^+ in this study (4.9 *a.u.*). In the literature the polarizability reported for potassium is 5.0 *a.u.*, a value very similar to that obtained in this work [25,26]. For the two binary systems, NaF-AlF_3 and KF-AlF_3, the polarizabilities of the fluorine obtained are very close, respectively 8.2 *a.u.* and 7.7 *a.u.*; this values remain in the expected range for molten fluorides (7.9 *a.u.*). The polarization of fluorine is affected by the

confinement effect of the potential linked to the local environment around fluoride ions. If the average value of the polarization for F^- reported is 7.9 *a.u.* for molten alkali fluorides, it has already been shown that this polarizability increases according to the alkaline size, from 7.8 to 11. 8 *a.u.* for LiF and CsF, respectively [20,25–27]. In conclusion, the small differences observed between the parameters obtained in this study and those already published depend on the studied system, the procedure of adjustment of the parameters and the number of configurations used during the adjustment. However, the parameters of the polarization and repulsion potential remain of the same order of magnitude as the values published for other fluoride alkaline. To build the interaction potential 13 configurations presented in table 2 were considered in order to cover a wide range of compositions for the system KF-AlF_3.

2.3 Calculations of NMR parameters

NMR parameters were calculated through the Density Functional Theory (DFT) implemented in CASTEP code [28,29]. Chemical shielding tensors were determined by the gauge including projector-augmented wave (GIPAW) method implemented in CASTEP. All calculations were done using ultra soft pseudopotentials (USPPs) "on-the-fly", and the Perdew, Burke, and Ernzerhof (PBE) functionals in the generalized gradient approximation (GGA). The cut-off energies were 610 eV and the Brillouin zone was sampled using k-point mesh of 1 × 1 × 1.

Throughout the trajectory of the molecular dynamic, 10 snapshots were extracted sufficiently spaced (every 100 ps) to ensure that they are uncorrelated [30]. For each snapshot, representing a given atomic configuration at time t, the individual chemical shielding of the different nuclei's from the system were calculated. In each snapshot for each nucleus, the isotropic screening tensor was averaged. Then this mean value has itself been averaged with all the other values obtained for the different snapshots extracted to obtain a single average value and its corresponding standard deviation. To convert the calculated isotropic chemical shielding into isotropic chemical shift, a linear regression between calculated σ_{iso} values and δ_{iso} experimental values established on numerous compounds by keeping the same calculation parameters obtained previously. For ^{19}F we use the relationship reported by Sadoc *et al.* [31], for ^{27}Al and ^{39}K, this relationship were made using our results: δ_{iso}=-1.0764*σ_{iso}(ppm)+590.84, δ_{iso}=-0.8436*σ_{iso}(ppm)+1026.9, respectively.

The isotropic chemical shift over the trajectory time represents the NMR signature for a given composition. This method has been proved to be an accurate way to simulate the high temperature NMR for molten salts [17]. As for the NaF-AlF_3 system [17], the chemical shifts for

the three nuclei (^{27}Al, ^{19}F and ^{39}K) where calculated for a wide range of concentrations of AlF_3.

3. Results and discussion

3.1 NMR chemical shifts : experimental and calculated

The quality of the potential can be assessed by comparing simulated physical quantities to experimental data. The validation of the potential was carried out through a direct comparison between calculated chemical shifts and those measured experimentally by NMR at high temperature.

The figure 1 reports the experimental chemical shift for ^{27}Al and ^{19}F nuclei recorded at 20°C above the melting point. Due to its low Larmor frequency (10.25 and 18.7 MHz at 9.4 T for the ^{39}K and ^{41}K isotopes respectively), it was not possible to observe the potassium signal with our high temperature NMR probe in this frequency range. Nevertheless, the comparison with the calculated values for the two nuclei (^{27}Al and ^{19}F) shows a very good agreement between the two set of data. The observed minor differences are included in the experimental error bars (few ppm). This experimental error was estimated from the width at half height of the peak and repeatability of measurements. Whatever the nucleus, the calculated values reproduce very well the evolution of the chemical shifts observed experimentally over a wide range of composition, between 5 to 50 mol. % AlF_3 and for a temperature above 975 K. Beyond this value the results should be analyzed with precaution, considering the probable sublimation of AlF_3.

The variation of the ^{39}K and ^{19}F chemical shifts with the AlF_3 concentration decreases monotonously whereas the ^{27}Al chemical shift increases in the same range. The evolution of ^{27}Al chemical shifts was explained in previous works [14,15,17] by the decrease of the Al coordination from 6 to 4 when the concentration of AlF_3 increases.

The ^{19}F chemical shift decreases with addition of AlF_3 and reach -190 ppm, which is assigned to fluoride incorporated in aluminum anionic complexes $[AlF_x]^{3-x}$. This good agreement between calculated and experimental chemical shifts shows the efficiency of the interatomic potential to describe the KF-AlF_3 molten system. It can be proved also with the good representation of molten density, figure 2 obtained by molecular dynamics simulations or experimentally at 1030°C. For this constant temperature, the density is close to a threshold value of 1.8 g/cm^3 for AlF_3 contents below 25 mol. % before decreasing in a monotonous way for higher concentrations.

3.2 Ionic coordination in the molten phase

To quantify the distribution of the $[AlF_x]^{3-x}$ species according to the amount of AlF_3, we used two methods. The first approach is derived from the chemical shift values measured experimentally by NMR and the second is based on calculations using the ionic trajectories from molecular dynamics simulations.

In molten media, the different ionic species present in the system are in very fast exchange (a few picoseconds), compared to the time scale of the NMR measurement (10^{-9} sec) [15,32]. Then, the high temperature NMR signal obtained results in a single lorentzian peak which is the time average of all ionic configurations. The averaged isotropic chemical shift ($\bar{\delta}$) associated with the peak position is the weighted average of the isotropic chemical shifts of each species $\delta^N(A_i)$ with their abundance (atomic fraction): $\bar{\delta} = \sum X_{Ai}^N . \delta^N(A_i)$, where $\delta^N(A_i)$ is the chemical shift for the nucleus *N* of the species A_i and X_{Ai}^N is the ratio between the number of nuclei *N* on the specie A_i and the total number of nuclei *N*.

As already described in previous works [14,15,17], it is possible to extract the anionic fractions of complexes from the evolution of the δ ^{19}F and ^{27}Al experimental chemical shifts, using the equations (1 and 2) with the chemical shift of each species (AlF_x^{3-x} and F^-) and the laws of mass conservation of :

$$\delta_F^{exp} = X_F^F . \delta_{F^-}^F + X_{AlF_6^{3-}}^F \delta_{AlF_6^{3-}}^F + X_{AlF_5^{2-}}^F \delta_{AlF_5^{2-}}^F + X_{AlF_4^-}^F \delta_{AlF_4^-}^F \quad (1)$$

$$\delta_{Al}^{exp} = X_{AlF_6^{3-}}^{Al} \delta_{AlF_6^{3-}}^{Al} + X_{AlF_5^{2-}}^{Al} \delta_{AlF_5^{2-}}^{Al} + X_{AlF_4^-}^{Al} \delta_{AlF_4^-}^{Al} \quad (2)$$

Where δ^{exp} represents the chemical shift measured inthe high temperature NMR experiments and X_j^i is the atomic fraction for the nucleus *i* and the anionic species *j*. However, it is necessary to know the value of the chemical shift of each species ($[AlF_x]^{3-x}$ and F^-) for ^{19}F and ^{27}Al nuclei in high temperature melts. We used some empirical correlation obtained by our previous experimental measurements and literature data [31,33–35].

Another method is based on the analysis of an ensemble of atomic configurations generated during the molecular dynamics simulations at a given temperature. To quantify the coordination of aluminum ions, we used the first RDF minimum (Al-F) identified as the radius of the first solvation sphere around each cation contained in the simulation box. To obtain a good counting statistic, the analysis was carried out on average on 10000 atomic configurations extracted at regular intervals on a dynamics of 1 nanosecond. This count gives

access to the atomic fraction of aluminum ions having 4, 5 or 6 fluorine neighbors to form $[AlF_x]^{3-x}$ anionic complexes.

Local information about fluoride ions can also be investigated through the number of bonds that fluorine has with aluminum ions. For this, the calculation is based on the comparison between the distances (F-F) and (Al-F) defined by the first minima of RDF (F-F) and (Al-F). We can then distinguish three types of fluoride ions: free fluorine when the fluorine ions are not connected to any aluminum, fluorine linked with an aluminum when they are engaged in monomers of the type $[AlF_x]^{3-x}$, and finally fluorine bound to two aluminum neighbors when bridging two monomers to form $[Al_2F_m]^{6-m}$ dimers.

The percentage of fluorine involved in complexes of the type $[AlF_x]^{3-x}$ increases with the AlF_3 concentration and the percentage of free fluorine decreases, as can be seen on figure 3. The existence of fluoride ions bound to two aluminum given $[Al_2F_m]^{6-m}$ dimers appears especially for contents higher than 25 mol. % of AlF_3. The atomic fraction of these dimers is less than 7 % for the sodium system and less than 2.5 % for the potassium system. This quantity of dimers nevertheless remains very negligible compared with the number of monomers. According to the low life time of Al-F-Al bonds (see the section *Dynamics of the anionic complexes*) the $[Al_2F_m]^{6-m}$ were not taken into account in the further analyses.

The resulting anionic fractions are shown in figure 4 for the KF-AlF_3 system and compared with the anionic fractions deduced from the high temperature NMR experiments. The uncertainty is estimated at ± 5 % on these anionic fractions after performing several tests on the parameters involved in molecular dynamics simulations (size box, number of configurations, spacing between each configurations,…). Over the wide range of composition the calculations reproduce very well the evolution of the free fluoride ions and $[AlF_x]^{3-x}$ species deduced from NMR and Raman spectroscopies [8]. Experiments and calculations confirm that the $[AlF_5]^{2-}$ species is predominant between 25 and 40 mol. % of AlF_3. For low AlF_3 concentration (< 25 mol. %), the averaged aluminum coordination in KF-AlF_3 system melts is lower than in NaF-AlF_3 melts, figure 5.

3.3 Thermodynamic model

In order to characterize the solubility of these molten salts, we calculate stoichiometric equilibrium constants for the dissociation reactions (I), (II) and (III) of the species (AlF_6^{3-}, AlF_5^{2-}, AlF_4^-) proposed to explain the evolution of these anionic complexes distributions. The equilibrium constant is defined by an operator of the chemical activities ($\propto_i$) of the chemical

species of the reaction: $K = \prod \left(\frac{\propto_i}{\propto_{ref}}\right)^{v}_{(eq)}$, where v means the stoichiometric algebra coefficient and $\propto_{ref}$ is the reference activity.

The chemical activity is defined as the active concentration of the species in solution. For an ideal solution, the chemical activity of species *i* is equal to its molar fraction (concentration). For dilute solutions, the solvent activity is 1 and the solute activity is taken as the ratio of the concentration of the species to a reference concentration. In a first step, we used this approximation to determine the stoichiometric equilibrium constants by taking the anionic fractions (x) obtained by the MD calculations and by the NMR, figure 6. The reference compounds are chosen according to the maximum concentration for each species: for M_3AlF_6 corresponds to a CR of 3, for M_2AlF_5 to a CR of 2 and for $MAlF_4$ to a CR of 1 (M=K or Na).

$$M_3AlF_6 \leftrightarrow M_2AlF_5 + MF \quad (I) \qquad K'_{65} = \frac{\propto_5^{ideal} . \propto_{MF}^{ideal}}{\propto_6^{ideal}} = \frac{x_5 . x_F}{x_6} . \frac{x_6^{ref}}{x_5^{ref} . x_{MF}^{ref}}$$

$$M_2AlF_5 \leftrightarrow MAlF_4 + MF \quad (II) \qquad K'_{54} = \frac{\propto_4^{ideal} . \propto_{MF}^{ideal}}{\propto_5^{ideal}} = \frac{x_4 . x_F}{x_5} . \frac{x_5^{ref}}{x_4^{ref} . x_{MF}^{ref}}$$

$$M_3AlF_6 \leftrightarrow MAlF_4 + 2MF \quad (III) \qquad K'_{64} = \frac{\propto_4^{ideal} . \propto_{MF}^{ideal\,2}}{\propto_6^{ideal}} = \frac{x_4 . x_F^2}{x_6} . \frac{x_6^{ref}}{x_4^{ref} . x_{MF}^{ref\,2}}$$

Where, M = Na, K

Note that the constant K'_{65} is greater than the constant K'_{54}, which proves the strong dissociation of the species $[AlF_6]^{3-}$ compared to that of the species $[AlF_5]^{2-}$. For high concentration of AlF_3, the constant K'_{54} increases because it is in this zone that the $[AlF_5]^{2-}$ species strongly dissociates in $[AlF_4]^-$. For the potassium system, the absence of variation of the equilibrium constants in the compositional range (5-35 mol. % AlF_3) confirms the "more ideal" behavior of this system compared to the system with NaF. This behavior can be explained by a weaker interaction of the anions with K^+ than with Na^+.

The real activity (a_i) is given as a function of the activity coefficient (γ) which represents the deviation of the activity of the real mixture with respect to this ideal solution:

$$a_i = \frac{c_i . \gamma_i}{c_{ref}^i} = a^{ideal} . \gamma_i$$

The real activities data were published by Solheim and Sterten [36] for $NaF-AlF_3$ system and are presented on FactSage software with the Vlab database [37] for $KF-AlF_3$ system. With the ideal activities obtained in this work by molecular dynamics and with the activities of Solheim and Sterten or FactSage for $NaF-AlF_3$ and $KF-AlF_3$ respectively, the activity coefficients for each species are obtained, Figure 7. The deviation of 1 indicates the non-ideality of these mixtures. This deviation is greater for $NaAlF_4$ ($1 \leq \gamma \geq 5$). For the NaF and Na_2AlF_5 the activity coefficients do not seem to vary and remain around 1, this had already been observed in E. Robert's thesis [38]. For $KF-AlF_3$ system, the activity coefficients have values very close to 1, which indicates an ideal behavior of the mixtures. Compared with the previous system, we can say that the $KF-AlF_3$ system is more ideal than the $NaF-AlF_3$ system.

3.4 Dynamics of the anionic complexes

The relaxation time of the first coordination sphere of Al^{3+} ions can be studied by means of cage correlation functions that make it possible to effectively account for the exchange dynamics of F^- ions between this sphere and the rest of the system. These autocorrelation functions were developed by Rabani et al. [39]. The autocorrelation function “out” representing the leaving of a fluorine ion is not the same that the “in-out” function that represents the modification of the Al solvation shell by either the entrance or the exit of one fluoride. This shows that the release of fluorine is not necessarily accompanied by the arrival of another ion for $MF-AlF_3$ systems (M=Na or K).

For both systems figure 8 reports the evolution of this relaxation time for the Al-F pairs as a function of the AlF_3 composition. Whatever the system, $NaF-AlF_3$ or $KF-AlF_3$, these times are very low, on the order of 10-20 ps, which is well beyond the measurement time of NMR (a few ms). However, it is always lower for the sodium system than for the potassium system, in agreement with the barrier energy results latter presented (figure 9). The exchanges between the fluorine and aluminum ions are "slower" on KF system which tends to stabilize a little more the species present in the liquid. Overall, the relaxation time decreases with AlF_3 concentration. This result is similar to our previous observations on zirconium-based molten fluorides [40].

The cage functions of the Al-Al pair were investigated in order to know the lifetime of the Al-F-Al link. The very short duration (between 0.3 and 0.1 ps for $NaF-AlF_3$ and 0 ps for $KF-AlF_3$) indicates the instability of the Al-F-Al bonds. This confirms the instability of formation

of a "network" consisting of $[AlF_x]^{3-x}$ monomers connected to each other via "bridging" fluorine ions to form $[Al_2F_m]^{6-m}$ dimers.

From a qualitative point of view, the RDF of the Al-F pair shows a narrow and very intense first peak, characteristic of a strong covalent and ionic interaction leading to the formation of well-defined coordination sphere (AlF_x^{3-x}). In addition, a well-marked minimum is observed with a very low value of g(r). This indicates that fluorine ions must cross a large barrier to exit the first solvation sphere of aluminum ions [41]. Comparing to NaF-AlF_3 system reported in previous work, the first peak of the RDF for the Na-F pair is much less intense and wider, which reveals a lesser structured first coordination sphere around the Na^+ and K^+ cations. The higher value of g(r) of the first minimum suggests that the exchange of sodium and potassium ions is easily done between the first and the second coordinating sphere of aluminum and fluorine ions.

The strength of the ionic bonds can be evaluated by the potential of mean force (PMF) [42] for the Na-F and K-F pairs. The barrier energy corresponding to the energy difference between the first maximum and the first minimum of the PMF, is higher for the sodium system (NaF-AlF_3), figure 9. This indicates that the fluorine ions contained in the sodium coordination sphere are more difficult to separate than when they are in the presence of potassium. In other words, for an identical temperature, the fact that the interaction between alkali-fluorine is stronger with sodium could go in the direction of greater dissociation of KF resulting in more free fluorine available in the molten phase. This result seems consistent with the qualitative fluoroacidity scale of different fluoride compounds proposed by Kergoat et al. [43]. The authors made reference to the fact that there is a relationship between the fluoroacidity based on free fluorides content in molten mixtures and the polarizability which reflects the electronic densities fluctuations of ions due to the interactions with their environment. When passing from one cation to another in the series $Li^+ < Na^+ < K^+ < Rb^+ < Cs^+$, the anion-cation distance increases, which results in an increase in F^- polarizability due to the diminution of the confining potential exerted on its electrons by its neighbors [27,44]. As the size of the alkali ion increases, the polarizability value tends to the free F^- anion polarizability (16 a. u.) suggesting a greater amount of free F^- and consequently a smaller fluoroacidity observed in these fluoride mixtures, according the qualitative fluoroacidity scale proposed by Bieber and Kergoat [43,45] . However, compared to the Al^{3+}-F^- barrier energy the M-F^- (M=Na or K) bond is very weak, figure 9. The difference in barrier energy between Na-F and K-F is mostly visible for acid cryolitic ratios (high AlF_3 concentrations) but this remains rather low. Finally, for the KF-

AlF_3 system, the Al-F barrier appears to be more difficult to overcome, which amounts to confirming the capacity of potassium to stabilize more the anionic species $[AlF_x]^{3-x}$ than sodium by slowing down the entrance and exit of the fluorine ions in the solvation sphere of aluminum.

3.5 Transport properties : viscosity, electrical conductivity and self-diffusion

Electrical conductivity is obtained from the mean square displacement of all atoms during the trajectory of 1 nanosecond from the MD simulations according the method explained in previous works [17]. For the KF-AlF_3 molten system only two measurements have been found in the literature. Both concern measurements made at liquidus temperature on a composition containing 40 mol. % of AlF_3 [46,47]. A good agreement for the electrical conductivity is obtained between the calculated values and the experimental measurements (figure 10).

Calculation show a decrease in electrical conductivity as the amount of AlF_3 increases in the system. Finally, the electrical conductivity in KF-AlF_3 system is lower than in NaF-AlF_3 system.

In the absence of an external electric field, the coefficients of self-diffusion of the ions subjected to a Brownian motion are easily accessible starting from the slope of the curve giving the evolution of the mean square displacement (MSD) of the ions taken individually as a function of time, according to the following relation: $D_\alpha = \lim_{t\to\infty} \frac{1}{6t}(|\delta r_i(t)|^2)$. The correction proposed by Yeh and Hummer [48] is also introduced to correct the effect of the periodic boundary conditions.

The calculated self-diffusion coefficients for each ion along the isotherm at 1305 K are shown in Figure 11. We compared them with measurements of self-diffusion coefficients obtained by M. Gobet [49] in the laboratory using a Pulsed Field Gradient NMR probe combined with laser heating [50], [18]. The agreement between calculated and measured values is very good. Since potassium ions are free (i.e. they do not participate in stable structural entities), their diffusion coefficients are higher than those of Al^{3+} and F^- ions. In the case of fluorine ions we can see that the diffusion coefficient decreases with the amount of AlF_3 and tends to converge towards that of aluminum ions. This is consistent with the structural analysis, which showed a decrease in the proportion of free fluorides in favor of an increasing involvement of fluorine in the $[AlF_x]^{3-x}$ complexes as the content in AlF_3 increases.

The viscosity is calculated using the Green-Kubo formalism from the temporal integral of the autocorrelation function obtained by molecular dynamics. For the viscosity a long trajectory

is necessary, for the calculations we use a trajectory of 5 nanoseconds. The viscosity increases with AlF_3 concentration (Figure 12) and is higher in the case of the sodium system [51]. These results are in agreement with the speciation, since the free fluorine decreases with AlF_3 content and the aluminum averaged coordination is lower in potassium system. As far as we know; no experimental results for viscosity have been published for KF-AlF_3 systems.

4. Conclusion

This work successfully developed a polarizable interaction potential to describe the molten system KF-AlF_3 over a wide range of composition by molecular dynamics simulations. The potential was tested by comparing the high temperature experimental chemical shifts obtained by NMR and those calculated ab initio by DFT. For this, we have implemented a protocol for extracting different atomic configurations from the MD in order to integrate the dynamics and the temperature of these systems into the calculation of the NMR parameters. The good representation of the chemical shifts is a very solid proof of the validation of the interaction potential used in the simulations. This validation is carried out in a wide range of composition, 0-50 mol. % in the molten state. Statistical analysis of ionic trajectories from molecular dynamics simulations allowed us to specify the speciation in these media according to the composition and temperature.

The speciation was determined experimentally by high temperature NMR and calculated by molecular dynamics simulations. The results obtained are in agreement with those determined by high temperature Raman in Gilbert's team. There is a majority of free fluorine up to 25 mol. % of AlF_3 then $[AlF_5]^{2-}$ species become the majority between 25 mol. % and 40 mol. % of AlF_3 with a maximum at 33 mol. % of AlF_3 (anionic fractions ≈ 60 %). Above 40 mol. %, the quantity of complexes $[AlF_4]^-$ becomes predominant. The proportion of $[AlF_6]^{3-}$ complexes remains very minor regardless of the AlF_3 composition.

This work also compares the results obtained for the two MF-AlF_3 binary systems (M = Na, K). The coordination of aluminum is lower in the potassium system for compositions lower than 20 mol. % of AlF_3. The knowledge of the anionic fractions allowed us to propose a mechanism of dissociation of the species present in the liquid and to calculate the equilibrium constants of the reactions involved and activity coefficients of the different species in molten MF-AlF_3 mixtures (M=Na or K). By accessing the dynamics of the liquid at the microscopic scale, we have been able to go back to the average lifetime of the species and have access to the transport properties such as the electrical conductivity and the self-diffusion coefficients. Regardless of the binary system, the life time of $[AlF_3]^{3-x}$ species is very short, between 25

and 5 ps. Dimer species of the type $[Al_2F_m]^{6-m}$ have a very low probability of existing (< 7 % for the NaF-AlF_3 system and < 3% for the KF-AlF_3 system) with high instability (bonding duration < 0.3 ps for the NaF-AlF_3 system and 0 ps for the KF-AlF_3 system).

The analysis of the average force potential for the Na-F and K-F pair, for an identical temperature, led to the conclusion that the cation-F^- (cation Na or K) interaction is stronger in the NaF-AlF_3 system. However, the alkaline-fluorine bond is very weak in comparison with the Al-F bond whatever the composition.

With regard to the transport properties, the increase in the ionic radius of the cation (Na → K) results in a decrease in the melting temperature, the density and the electrical conductivity of the molten baths. Coupling HT NMR measurements, molecular dynamics and DFT calculations have proven to be a powerful approach for the study of fluorinated molten salts.

Acknowledgements

This study was financially supported by the ANR MIMINELA project of the French National Research Agency. For the MD and DFT calculations, we thank the "Centre de Calcul Scientifique en Région Centre" (CCSC, Orléans, France) and particularly F. Vivet and L. Catherine for their technical support during the computations. We would also like to thank Dr E. Robert for his contribution concerning the activity coefficients calculations.

References

(1) Robert, E.; Olsen, J. E.; Daněk, V.; Tixhon, E.; Ostvold, T.; Gilbert, B. Structure and Thermodynamics of Alkali Fluoride-Aluminum Fluoride-Alumina Melts. Vapor Pressure, Solubility, and Raman Spectroscopic Studies. *J. Phys. Chem. B* 1997, *101* (46), 9447–9457.

(2) Ishii, Y.; Sato, K.; Salanne, M.; Madden, P. A.; Ohtori, N. Thermal Conductivity of Molten Alkali Metal Fluorides (LiF, NaF, KF) and Their Mixtures. *J. Phys. Chem. B* 2014, *118* (12), 3385–3391.

(3) Alexei Apisarov, A. D. Liquidus Temperatures of Cryolite Melts With Low Cryolite Ratio. *Metall. Mater. Trans. B* 2010, *42* (1), 236–242.

(4) Cassayre, L.; Palau, P.; Chamelot, P.; Massot, L. Properties of Low-Temperature Melting Electrolytes for the Aluminum Electrolysis Process: A Review. *J. Chem. Eng. Data* 2010, *55* (11), 4549–4560.

(5) Thonstad, J.; Fellner, P.; Haarberg, G. M.; Híveš, J.; Kvande, H.; Sterten, Å. *Aluminium Electrolysis, Fundamentals of the Hall-Heroult Process*, 3rd ed.; Aluminium-Verlag, 2001.

(6) Apisarov, A. P.; Dedyukhin, A. E.; Red'kin, A. A.; Tkacheva, O. Y.; Zaikov, Y. P. Physicochemical Properties of KF-NaF-AlF3 Molten Electrolytes. *Russ. J. Electrochem.* 2010, *46* (6), 633–639.

(7) Galasiu, I.; Galasiu, R.; Thonstad, J. *Inert Anodes for Aluminium Electrolysis*, 1st ed.; Aluminium-Verlag: Dusseldorf, 2007.

(8) Tixhon, E.; Robert, E.; Gilbert, B. Molten Kf-Aif(3) System - a Study by Raman-Spectroscopy. *Appl. Spectrosc.* 1994, *48* (12), 1477–1482.
(9) Li, J.; Fang, Z.; Lai, Y.; Lü, X.; Tian, Z. Electrolysis Expansion Performance of Semigraphitic Cathode in [K3AlF6/Na3AlF6]-AlF3-Al2O3 Bath System. *J. Cent. South Univ. Technol.* 2009, *16* (3), 422–428.
(10) Phillips, B.; Warshaw, C. M.; Mockrin, I. Equilibria in KFAlF4-Containing Systems. *Am. Ceram. Soc.* 1966, *49 (12)*, 631–634.
(11) Pushin, N. A.; Baskov, A. V. 1913, *135 (82)*.
(12) Jenssen, B. Phase and Structure Determination of New Complex Alkali Aluminum Fluoride, The University of Tronfheim: Norway, 1969.
(13) Gilbert, B.; Robert, E.; Tixhon, E.; Olsen, J. E.; Ostvold, T. Structure and Thermodynamics of NaF-AlF3 Melts with Addition of CaF2 and MgF2. *Inorg. Chem.* 1996, *35* (14), 4198–4210.
(14) Lacassagne, V.; Bessada, C.; Florian, P.; Bouvet, S.; Ollivier, B.; Coutures, J. P.; Massiot, D. Structure of High-Temperature NaF-AlF3-Al2O3 Melts: A Multinuclear NMR Study. *J. Phys. Chem. B* 2002, *106* (8), 1862–1868.
(15) Nuta, I.; Veron, E.; Matzen, G.; Bessada, C. High Temperature NMR Study of Aluminum Metal Influence on Speciation in Molten NaF-AIF(3) Fluorides. *Inorg. Chem.* 2011, *50* (8), 3304–3312.
(16) Robert, E.; Olsen, J. E.; Gilbert, B.; Ostvold, T. Structure and Thermodynamics of Potassium Fluoride Aluminium Fluoride Melts. Raman Spectroscopic and Vapour Pressure Studies. *Acta Chem. Scand.* 1997, *51* (3), 379–386.
(17) Machado, K.; Zanghi, D.; Sarou-Kanian, V.; Cadars, S.; Burbano, M.; Salanne, M.; Bessada, C. Study of NaF–AlF3 Melts by Coupling Molecular Dynamics, Density Functional Theory, and NMR Measurements. *J. Phys. Chem. C* 2017, *121* (19), 10289–10297.
(18) Rollet, A.-L.; Sarou-Kanian, V.; Bessada, C. Self-Diffusion Coefficient Measurements at High Temperature by PFG NMR. *Comptes Rendus Chim.* 2010, *13* (4), 399–404.
(19) Bonafous, L.; Ollivier, B.; Auger, Y.; Chaudret, H.; Bessada, C.; Massiot, D.; Coutures, J. P. *J Chim Phys* 1995, *92*, 1867–1870.
(20) Salanne, M.; Madden, P. A. Polarization Effects in Ionic Solids and Melts. *Mol. Phys.* 2011, *109* (19), 2299–2315.
(21) Madden, P. A.; Wilson, M. 'Covalent' Effects in 'Ionic' Systems. *Chem Soc Rev* 1996, *25* (5), 339–350.
(22) Hutchinson, F.; Wilson, M.; Madden, P. A. A Unified Description of MCl_3 Systems with a Polarizable Ion Simulation Model. *Mol. Phys.* 2001, *99* (10), 811–824.
(23) Kresse, G.; Furthmüller, J. Efficiency of Ab-Initio Total Energy Calculations for Metals and Semiconductors Using a Plane-Wave Basis Set. *Comput. Mater. Sci.* 1996, *6* (1), 15–50.
(24) Kresse, G.; Furthmüller, J. Efficient Iterative Schemes for *Ab Initio* Total-Energy Calculations Using a Plane-Wave Basis Set. *Phys. Rev. B* 1996, *54* (16), 11169–11186.
(25) Salanne, M.; Rotenberg, B.; Jahn, S.; Vuilleumier, R.; Simon, C.; Madden, P. A. Including Many-Body Effects in Models for Ionic Liquids. *Theor. Chem. Acc.* 2012, *131* (3), 1–16.
(26) Ghetta, V.; Fouletier, J.; Taxil, P. *Sels fondus à haute température*, Première édition.; Presses Polytechniques et Universitaires Romandes: Lausanne, 2009.
(27) Salanne, M. Simulations of Room Temperature Ionic Liquids: From Polarizable to Coarse-Grained Force Fields. *Phys Chem Chem Phys* 2015, *17* (22), 14270–14279.

(28) Clark, S. J.; Segall, M. D.; Pickard, C. J.; Hasnip, P. J.; Probert, M. I. J.; Refson, K.; Payne, M. C. First Principles Methods Using CASTEP. *Z. Für Krist. - Cryst. Mater.* 2009, *220* (5/6), 567–570.
(29) Segall, M. D.; Lindan, P. J. D.; Probert, M. J.; Pickard, C. J.; Hasnip, S. J.; Clark, S. J.; Payne, M. C. First-Principles Simulation: Ideas, Illustrations and the CASTEP Code - IOPscience. *J. Phys. Condens. Matter* 2002, *14* (11).
(30) Robinson, M.; Haynes, P. D. Dynamical Effects in *Ab Initio* NMR Calculations: Classical Force Fields Fitted to Quantum Forces. *J. Chem. Phys.* 2010, *133* (8), 084109.
(31) Sadoc, A.; Body, M.; Legein, C.; Biswal, M.; Fayon, F.; Rocquefelte, X.; Boucher, F. NMR Parameters in Alkali, Alkaline Earth and Rare Earth Fluorides from First Principle Calculations. *Phys. Chem. Chem. Phys.* 2011, *13* (41), 18539.
(32) Lacassagne, V.; Bessada, C.; Ollivier, B.; Massiot, D.; Florian, P.; Coutures, J. P. Al-27, Na-23, F-19 NMR study of cryolife at the solid/liquid transition. *Comptes Rendus Acad. Sci. Ser. Ii Fasc. B-Mec. Phys. Chim. Astron.* 1997, *325* (2), 91–98.
(33) Auguste, F. Etude Par Spectroscopie Raman et de Résonance Magnétique Nucléaire de l'Effet de La Température Sur Le Comportement et La Structure Des Fluoraluminates Alcalins, Université de Liège: Liège, Belgique, 2003.
(34) Kohn, S. C.; Dupree, R.; Mortuza, M.; Henderson, C. M. B. NMR Evidence for 5-Coordinated and 6-Coordinated Aluminum Fluoride Complexes in F-Bearing Aluminosilicate Glasses. *Am. Mineral.* 1991, *76*, 309–312.
(35) Sadoc, A.; Biswal, M.; Body, M.; Legein, C.; Boucher, F.; Massiot, D.; Fayon, F. NMR Parameters in Column 13 Metal Fluoride Compounds (AlF3, GaF3, InF3 and TlF) from First Principle Calculations. *Solid State Nucl. Magn. Reson.* 2014, *59–60*, 1–7.
(36) Solheim, A.; Sterten, Å. Activity Data for the System NaF-AlF3. *Ninth Int. Symp. Light Met. Prod. Tromsø-Trondheim Nor.* 1997, 225–34.
(37) Bale, C. W.; Chartrand, P.; Degterov, S. A.; Eriksson, G.; Hack, K.; Ben Mahfoud, R.; Melançon, J.; Pelton, A. D.; Petersen, S. FactSage Thermochemical Software and Databases. *Calphad* 2002, *26* (2), 189–228.
(38) Robert, E. A Structural and Thermodynamic Study of Fluoroaluminate Molten Salt, Université de Liège: Liège, Belgique, 1998.
(39) Rabani, E.; Gezelter, J. D.; Berne, B. J. Calculating the Hopping Rate for Self-Diffusion on Rough Potential Energy Surfaces: Cage Correlations. *J. Chem. Phys.* 1997, *107* (17), 6867–6876.
(40) Pauvert, O.; Salanne, M.; Zanghi, D.; Simon, C.; Reguer, S.; Thiaudiere, D.; Okamoto, Y.; Matsuura, H.; Bessada, C. Ion Specific Effects on the Structure of Molten AF-ZrF4 Systems (A(+) = Li+, Na+, and K+). *J. Phys. Chem. B* 2011, *115* (29), 9160–9167.
(41) Corradini, D.; Madden, P. A.; Salanne, M. Coordination Numbers and Physical Properties in Molten Salts and Their Mixtures. *Faraday Discuss.* 2016, *190* (0), 471–486.
(42) Hansen, J.-P.; McDonald, I. R. *Theory of Simple Liquids*, 3rd Edition.; Academic Press: New York, 2006.
(43) Kergoat, M.; Massot, L.; Gibilaro, M.; Chamelot, P. Investigation on Fluoroacidity of Molten Fluorides Solutions in Relation with Mass Transport. *Electrochimica Acta* 2014, *120*, 258–263.
(44) Salanne, M.; Vuilleumier, R.; Madden, P. A.; Simon, C.; Turq, P.; Guillot, B. Polarizabilities of Individual Molecules and Ions in Liquids from First Principles. *J. Phys. Condens. Matter* 2008, *20* (49), 494207.

(45) Bieber, A. L.; Massot, L.; Gibilaro, M.; Cassayre, L.; Chamelot, P.; Taxil, P. Fluoroacidity Evaluation in Molten Salts. *Electrochimica Acta* 2011, *56* (14), 5022–5027.
(46) Palimaka, P.; Pietrzyk, S. Research on the Electrical Conductivity of of Fluoride Electrolytes NaF-AlF3-CaF2 in Liquid and Solid State. *Arch. Metall. Mater.* 2014, *59* (1), 71–75.
(47) Yang, J.; Li, W.; Yan, H.; Liu, D. Conductivity of KF-NaF-AlF3 System Low-Temperature Electrolyte. *Light Met.* 2013, 689–693.
(48) Yeh, I.-C.; Hummer, G. System-Size Dependence of Diffusion Coefficients and Viscosities from Molecular Dynamics Simulations with Periodic Boundary Conditions. *J. Phys. Chem. B* 2004, *108* (40), 15873–15879.
(49) Gobet, M.; Sarou-Kanian, V.; Rollet, A.-L.; Salanne, M.; Simon, C.; Bessada, C. Transport Properties in Cryolitic Melts: NMR Measurements and Molecular Dynamics Calculations of Self-Diffusion Coefficients. *Molten Salts Ion. Liq. 17* 2010, *33* (7), 679–684.
(50) Sarou-Kanian, V.; Rollet, A.-L.; Salanne, M.; Simon, C.; Bessada, C.; Madden, P. A. Diffusion Coefficients and Local Structure in Basic Molten Fluorides: In SituNMR Measurements and Molecular Dynamics Simulations. *Phys. Chem. Chem. Phys.* 2009, *11* (48), 11501–11506.
(51) Brockner, W.; Tørklep, K.; Øye, H. A. Viscosity of Sodium Fluoride-Aluminium Fluoride Melt Mixtures. *Berichte Bunsenges. Für Phys. Chem.* 1979, *83* (1), 12–19.

Table 1 : Potential parameters for the KF-AlF_3 system (all parameters are given in atomic units (*a.u.*)) The polarizability obtained for the fluorine and potassium nuclei is 7.7 *a.u.* and 4.9 *a.u.* respectively. For aluminum, the polarizability has been set to zero.

Pair of ions	B_{ij}	α_{ij}	C_{ij}^{6}	C_{ij}^{8}	b^{ij}	c_D^{ij}	b_D^{ij}
$F^- - F^-$	124,8	2,2	16,4	10,0	1,9	0,4	1,9
$F^- - Al^{3+}$	34,6	1,8	0,5	66,2	1,9	1,6	2,0
$F^- - K^+$	58,7	1,8	45,8	56,1	1,9	2,0	1,6
$Al^{3+} - Al^{3+}$	7,6 E-4	7,8	98,2	781,5	2,2	-0,3	1,6
$Al^{3+} - K^+$	1,1	9,5	60,0	800,0	1,9	0	10
$K^+ - K^+$	150,0	2,0	60,0	500,0	1,9	0	10

Table 2 : Molecular dynamics simulations conditions.

N°	mol. % AlF_3	N_{F-}	N_{K+}	N_{Al3+}	Volume $Å^3$
1	5	115	100	5	3426
2	10	124	94	10	3450
3	15	138	90	16	3405
4	20	148	85	21	3536
5	25	120	60	20	3543
6	28	122	56	22	3609
7	29	120	54	22	3726
8	31	124	52	24	4182
9	33	125	50	25	4025
10	37	126	45	27	2989
11	39	128	44	28	3954
12	45	131	38	31	4035
13	50	132	33	33	4215

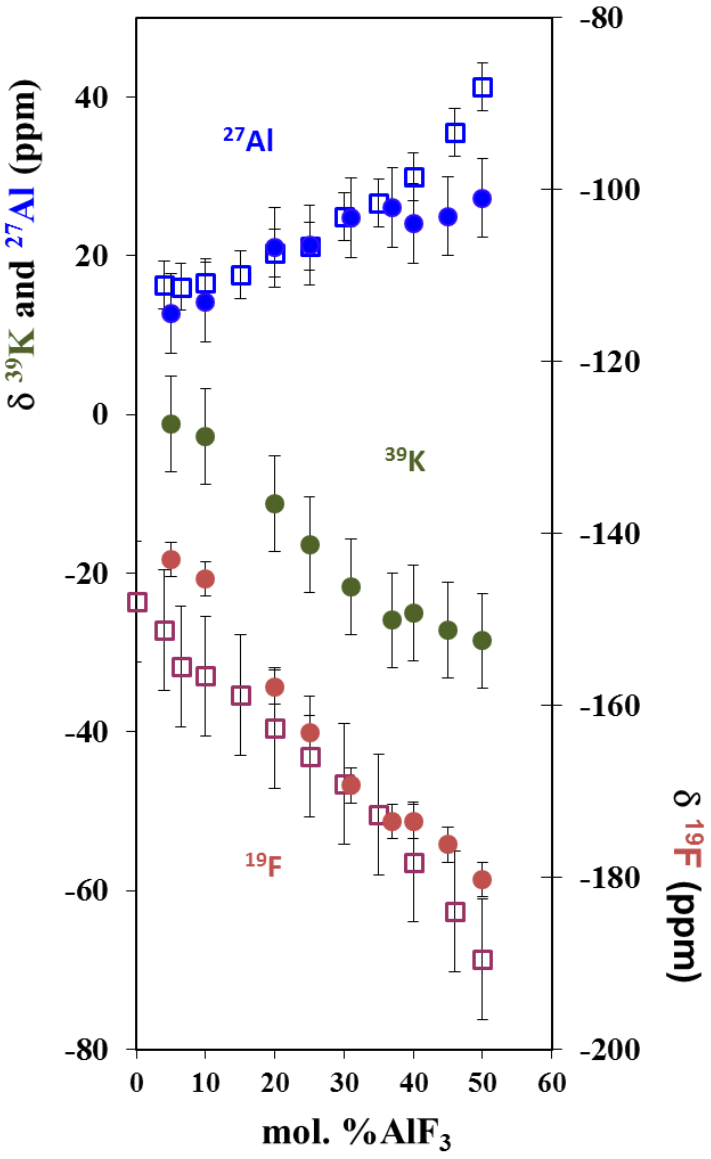

Figure 1 : Comparison of the calculated chemical shifts (solid markers) and measured (empty markers) on molten system as a function of mol. % AlF_3.

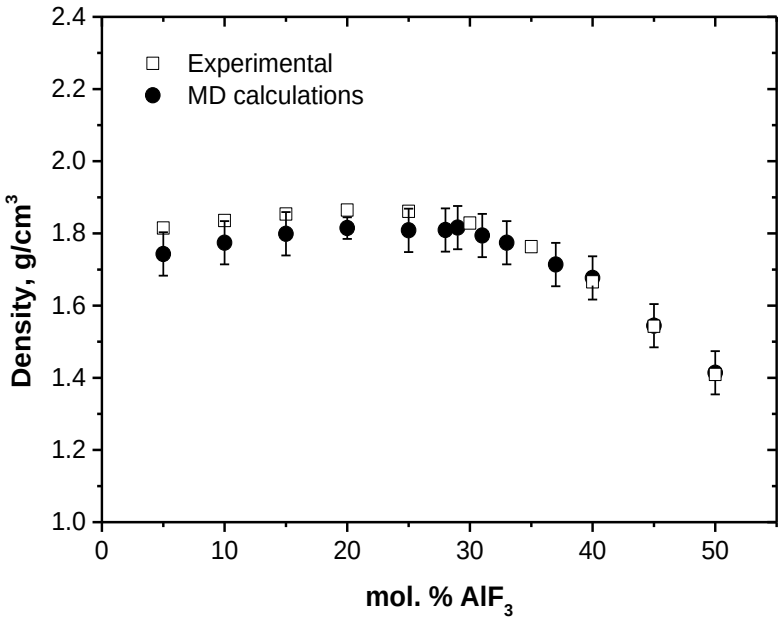

Figure 2 : Density of KF-AlF_3 molten baths obtained by molecular dynamics simulations (●) and experimentally by C.W.Bale [37] (□) at 1305 K.

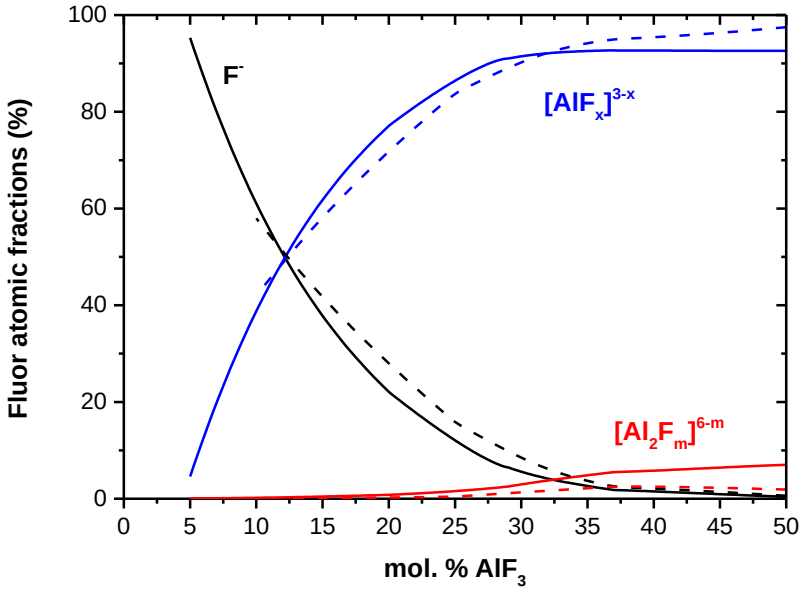

Figure 3 : Atomic fractions of fluorine: free fluorine (black); fluorine bridging aluminum (blue) and bridging fluorine two aluminum (red) depending on mol. % AlF_3 at 1305 K for systems: NaF-AlF_3 (line) and KF-AlF_3 (dotted line).

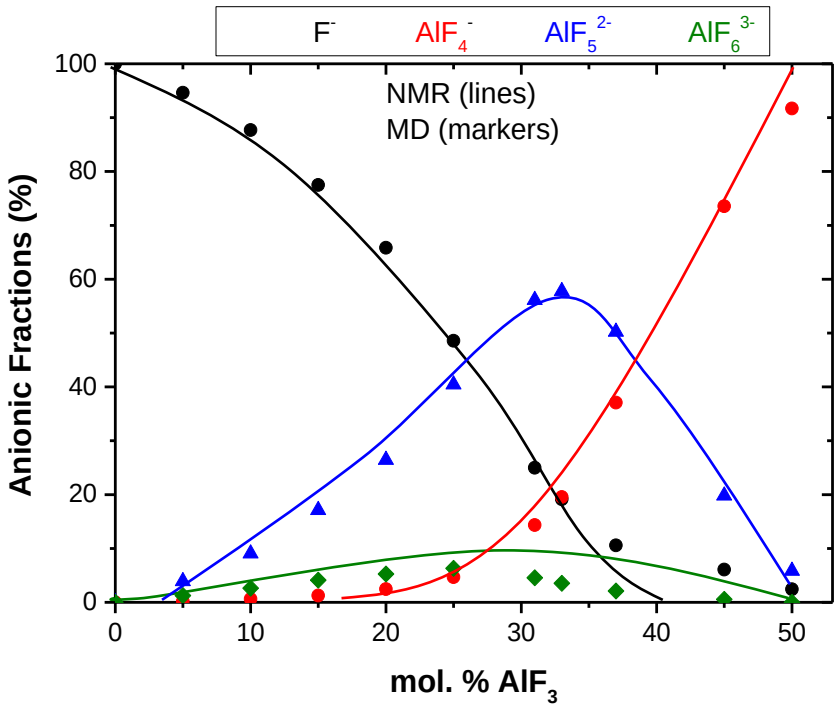

Figure 4 : Anionic fractions of the KF-AlF_3 system deduced from NMR (line) experiments at constant superheat temperature and molecular dynamics (markers) at 1305 K.

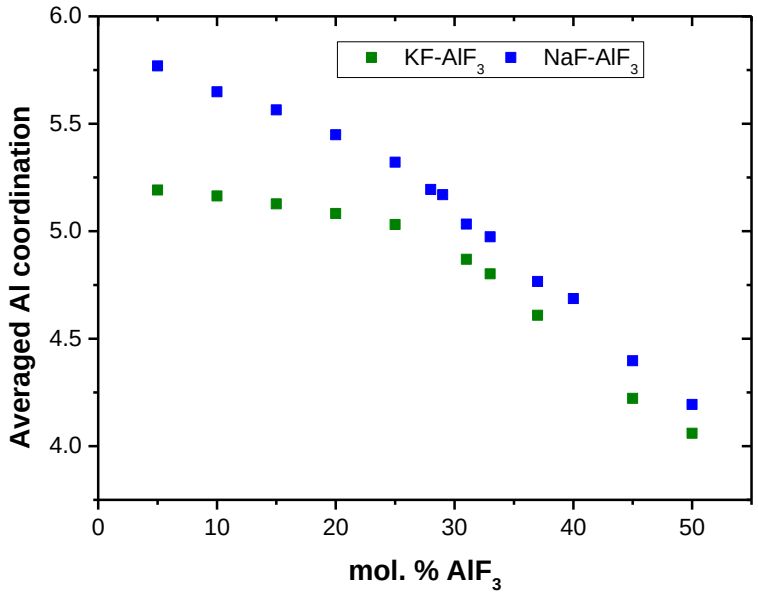

Figure 5 : Average coordination of aluminum in MF-AlF_3 melt baths (M = Na, K) obtained by molecular dynamics calculations at 1305 K.

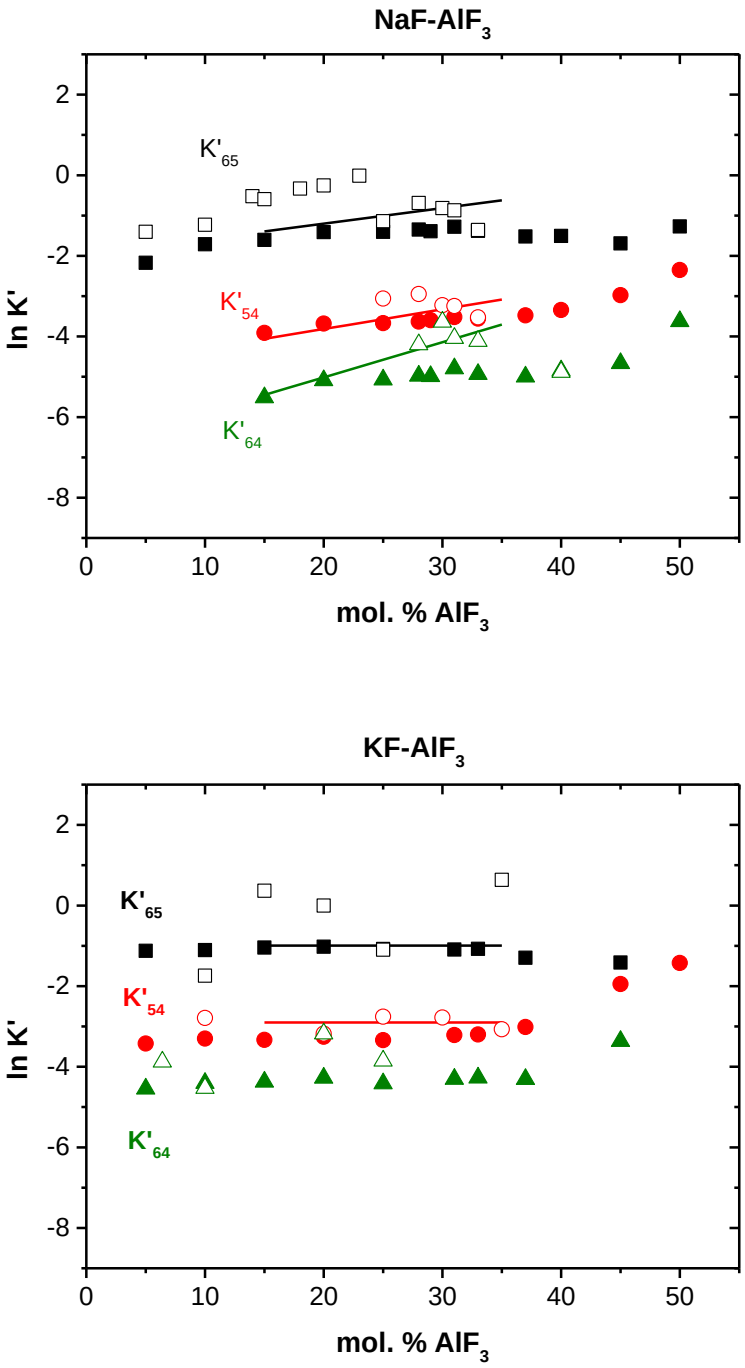

Figure 6 : Equilibrium constants for MF-AlF_3 systems (M = Na or K) calculated at 1305 K (solid markers), compared with those deduced from Raman measurements at 1293 K (line) [38] and by NMR (empty markers).

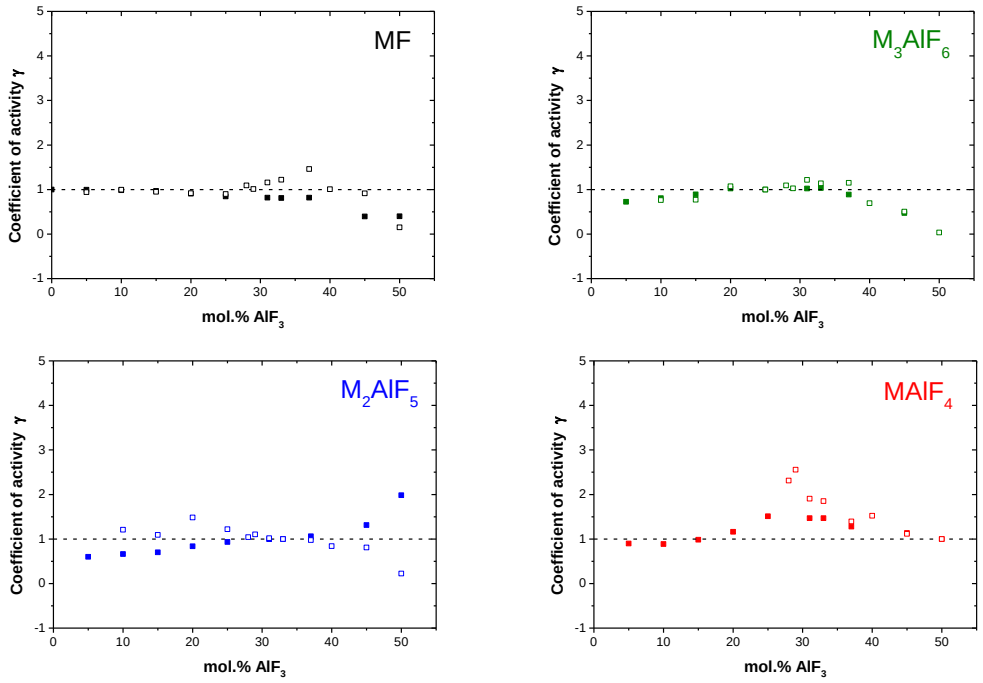

Figure 7 : Activity coefficients calculated for each species (MF, M_3AlF_6, M_2AlF_5 and AlF_5 with M= K or Na) as a function of mol. % AlF_3 in KF-AlF_3 (empty markers) and NaF-AlF_3 (full markers) systems.

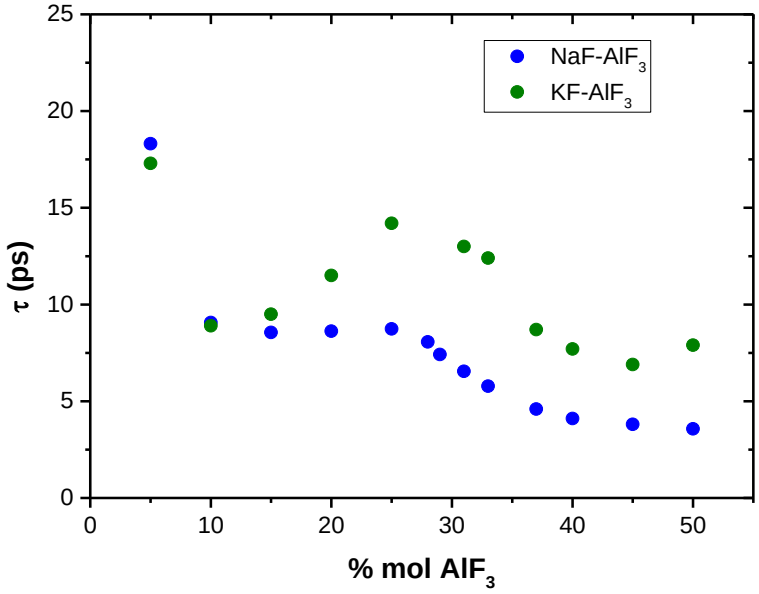

Figure 8 : Cage relaxation time for the Al^{3+} - F^- pair as a function of the AlF_3 concentration at 1305 K for the NaF-AlF_3 system (●) and KF-AlF_3 (●).

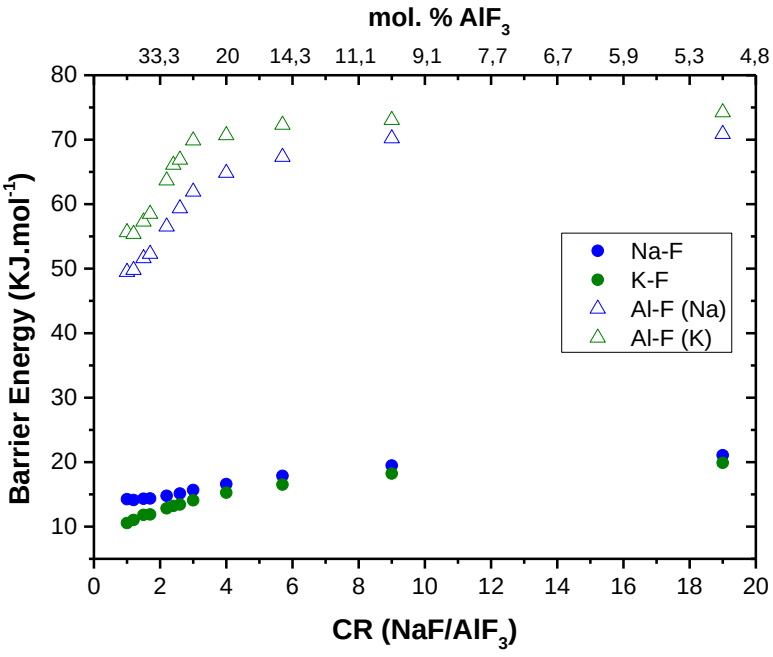

Figure 9 : Barrier energy at 1305 K for the alkaline-fluorine (●●) and Al^{3+} -F^- pair (ΔΔ)as a function of composition in the NaF-AlF_3 (●Δ) and KF-AlF_3 (●Δ) systems.

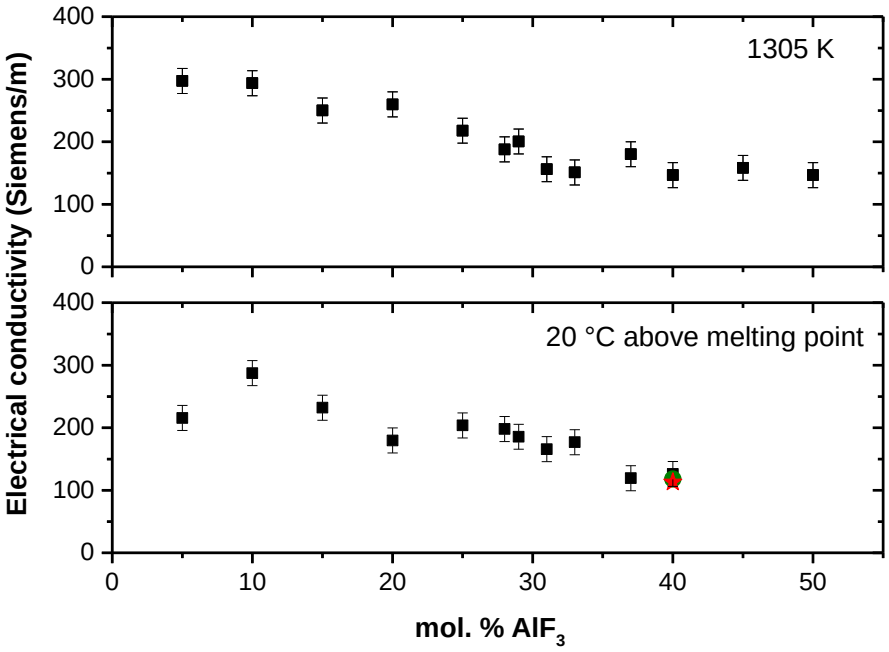

Figure 10 : Electrical conductivity of molten KF-AlF_3 from molecular dynamic calculations (■) and experimental data (★[46], ● [47]).

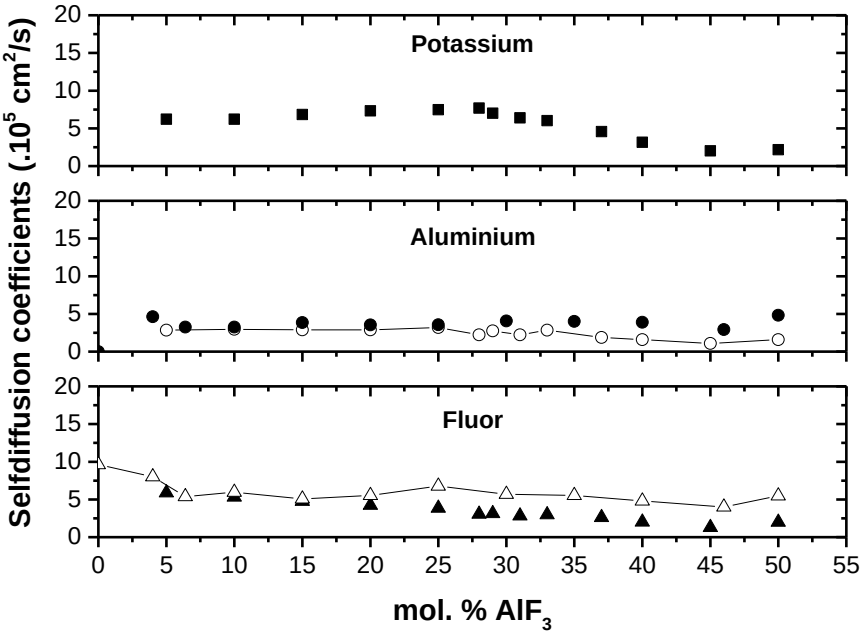

Figure 11 : Self-diffusion coefficients of potassium (squares), aluminum (circles) and fluorine ions (triangles) in KF-AlF_3 at 1305 K versus mol. % AlF_3. The solid symbols indicate

the results from the molecular dynamics simulation and the empty symbols the experimental data obtained by high temperature NMR [48].

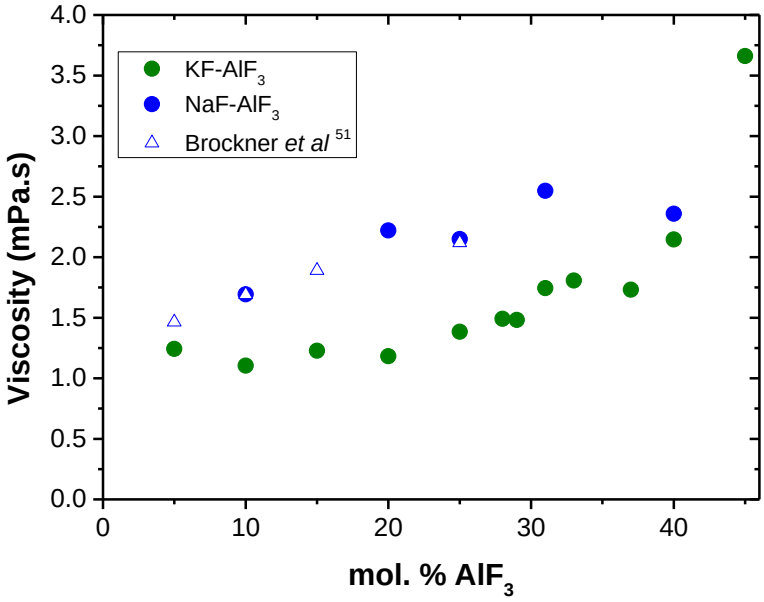

Figure 12 : Experimental [51] and calculated viscosity by the Green-Kubo formalism from 5 nanosecond molecular dynamics simulation 20°C above melting point for : $KF\text{-}AlF_3$ (●) and $NaF\text{-}AlF_3$ (●).